Published in final edited form as:
Lasers Surg Med. 2010 April ; 42(4): 306–312. doi:10.1002/lsm.20915.

Preliminary Investigation on Use of High-Resolution Optical Coherence Tomography to Monitor Injury and Repair in the Rat Sciatic Nerve

Cara A. Chlebicki, BA[1], **Alice D. Lee, MD**[1,2], **Woonggyu Jung, PhD**[1], **Hongrui Li, BS**[1], **Lih-Huei Liaw, MS**[1], **Zhongping Chen, PhD**[1], and **Brian J. Wong, MD, PhD**[1,2,*]

[1] Beckman Laser Institute and Medical Clinic, University of California-Irvine, 1002 Health Sciences Road East, Irvine, California 92612

[2] Department of Otolaryngology, Head and Neck Surgery, University of California-Irvine, 101 The City Drive, Orange, California 92668

Abstract

Background and Objective—Optical coherence tomography (OCT) has been used in limited settings to study peripheral nerve injury. The purpose of the study is to determine whether high-resolution OCT can be used to monitor nerve injury and regeneration in the rat sciatic nerve following crush injury, ligation, and transection with microsurgical repair.

Study Design/Materials and Methods—Forty-five rats were segregated into three groups. The right sciatic nerve was suture ligated (n = 15), cut then microsurgically repaired (n = 15), or crushed (n = 15). The left sciatic nerve served as the control; only surgical exposure and skin closure were performed. Each group was further divided into three subgroups where they were assigned survival durations of 4, 15, or 24 weeks. Following euthanasia, nerves were harvested, fixed in formalin, and imaged at the injury site, as well as proximal and distal ends. The OCT system resolution was approximately 7 μm in tissue with a 1,060 nm central wavelength.

Results—Control (uninjured) nerve tissue showed homogenous signal distribution to a relatively uniform depth; in contrast, damaged nerves showed irregular signal distribution and intensity. Changes in signal distribution were most significant at the injury site and distal regions. Increases in signal irregularity were evident during longer recovery times. Histological analysis determined that OCT imaging was limited to the surrounding perineurium and scar tissue.

Conclusion—OCT has the potential to be a valuable tool for monitoring nerve injury and repair, and the changes that accompany wound healing, providing clinicians with a non-invasive tool to treat nerve injuries.

Keywords

nerve injury; peripheral nerve; optical coherence tomography and nerve

[*]Correspondence to: Brian J. Wong, MD, PhD, Beckman Laser Institute and Medical Clinic, University of California-Irvine, 1002 Health Sciences Road East, Irvine, CA 92612. bjwong@uci.edu.

Presented at the 28th Annual Conference of the American Society for Laser Medicine and Surgery, Orlando, FL, April 2–6, 2008.

INTRODUCTION

Injury to peripheral nerves results from physical trauma, systemic diseases, toxins, and inflammation. Blunt, penetrating, or crush injuries to peripheral nerves may lead to immediate loss of sensory and/or motor function, often requiring surgical repair. The physiological processes associated with nerve injury and repair encompass a complex series of events including Wallerian degeneration, segmental demyelination, axonal sprouting, and regeneration [1–5].

Microsurgical repair of severed nerves is technically demanding, requiring the meticulous approximation of the proximal and distal nerve segments. Methods to monitor the regeneration process rely upon clinical observation of gross functional recovery (e.g., return of motor or sensory function) or electrophysiologic studies such as electromyography (EMG) and/or nerve conduction velocity (NCV) studies. Currently there are no clinical methods that provide detailed images of the injury and repair process without a biopsy. Imaging the structure of peripheral nerves in vivo would have value in research studies as this may potentially reduce the number of animal subjects euthanized for specimen procurement. Clinically, several disease processes such as diabetes occasionally require nerve biopsy to monitor the extent or progression of disease. In vivo imaging may obviate the need to perform a biopsy in many circumstances, as small incisions and minimally invasive techniques could be used to expose peripheral nerves and allow access for imaging. Optical coherence tomography (OCT) is a high-resolution imaging modality that may potentially be used to accomplish this task. Although similar in functionality to ultrasound technology, OCT utilizes a low-coherence light source rather than sound waves to detect variations in tissue. The broadband near-infrared light combined with a fiber optic Michelson interferometer allows the OCT system to produce cross-sectional images where image contrast is generated by differences in tissue optical properties [6]. OCT has several advantages over the other imaging and microscopy techniques in that it provides high-resolution cross-sectional images of living tissues without the need for cytotoxic fixation. Hence, OCT may have value as a research tool to study nerve injury repair and potentially have value in clinical management of neuropathic diseases as well.

To date, few studies have examined the use of OCT to image peripheral nerves, and most OCT nerve research has centered on ophthalmic applications primarily focused on imaging optic disc pathology, primarily in disease states such as glaucoma. This pilot study evaluated the use of high-resolution OCT to monitor the process of peripheral nerve regeneration following three forms of traumatic injury: crush injury, suture ligation, and nerve section with microsurgical repair.

MATERIALS AND METHODS

Forty-five adult male Sprague–Dawley rats (0.3–0.325 kg) were equally segregated into three experimental groups: suture ligation, section with microsurgical repair, and crush injury. Each group was further divided into three subgroups assigned survival durations of 4, 15, or 24 weeks. For all procedures the right sciatic nerve served as the experimental and the left as the control. The protocol was approved by the UC Irvine Institutional Animal Care and Use Committee (IACUC).

Animal Surgery

Animals were anesthetized with ketamine (75–100 mg/kg) and xylazine (10 mg/kg) administered intraperitoneally. The right thigh was shaved, sterilely prepped, and draped. A 2-cm long incision was carefully made to the buttock through the gluteal muscles exposing the sciatic nerve. For the ligation procedure, the sciatic nerve was sharply transected with a scalpel followed by ligation of the two severed ends with sutures. The ligated stumps were not

approximated. For microsurgical repair subjects, the severed ends of the nerve were re-approximated with sutures (8–0 polypropylene suture) using a dissection microscope to visualize the tissue. Finally, during the crush injury, the sciatic nerve was compressed three times consecutively with a clamp. In all three cases, the skin incisions were closed with non-absorbable suture. The left sciatic nerve (control) only underwent exposure followed by immediate skin closure. The total time for each procedure, including anesthetic induction, took approximately 45 minutes. Following surgery, the animals were monitored until fully recovered from anesthesia, and then returned to the vivarium.

Once the animals reached their assigned survival times, the rats were euthanized (pentobarital sodium, 150 mg/kg, i.p.). Meticulous microsurgical dissection was then performed to carefully harvest the sciatic nerves. The proximal and distal ends were identified and stabilized on cork squares where they were fixed in 10% formalin solution for 24 hours, and then rinsed and placed in a phosphate buffer (pH 7.4) solution for storage at 4°C.

Imaging

The nerves were imaged using the fiber-based time domain OCT system located at the Beckman Laser Institute. An OCT system at 1,060 nm center wavelength with approximately 7 μm resolution in tissue was chosen over other wavelengths because of its ability to penetrate further in tissue while still balancing resolution quality. Figure 1 shows a schematic of the fiber-based OCT system.

In the reference arm, a rapid-scanning optical delay line was used. The delay line consisted of a grating and curved mirror to produce spectral dispersion [7]. A Galvano mirror in the Fourier plane was angle scanned at high speed with an axial line scanning rate of 500 Hz. In order to match the dispersion induced between two paths, two pairs of prisms made of SF11 and a Lakn22 glass rod with 5 cm length were inserted in the delay line. Figure 2B,C shows the measured interferogram before/after dispersion compensation.

The reflected light from two paths was recombined and detected on a photodetector. The interference signal was observed only when the optical path length difference between sample and reference arms was less than the coherence length of the source. The detected optical interference fringe intensity signals were bandpass-filtered at the carrier frequency. Resultant signals were then digitized with an analog–digital converter and transferred to a computer where the structural image was generated.

Both control and experimental specimens were imaged at three locations: (1) the injury site (mid); (2) proximal to the injury site (presumably populated by normal axons); and (3) distal to the injury site (regenerating axons that traversed the region of injury). Proximal and distal scanning occurred approximately 5 mm from the injury site. All specimens were scanned 1 mm × 3 mm. Extensive analysis was conducted on all OCT images to determine the presence of variations in signal intensity and distribution which correlated with nerve structures.

Histology

After OCT imaging the nerve tissue samples were prepped for histology sectioning. The nerves were dehydrated in increasing concentrations of ethanol, rinsed with Histoclear (National Diagnostics, Manville, NJ), and saturated with paraffin in an ATPI tissue processor (Triangle Biomedical Sciences, Inc., Durham, NC). After dehydration the tissue samples were embedded in paraffin and allowed to set. Careful 6 μm serial sectioning was performed at the location on the nerve specimen where OCT imaging was conducted in order to have adequate section numbers to obtain registry with the OCT images. Once the sections were placed on 50%

Albumin Fixative coated glass slides, the tissue was deparaffinized with Histoclear and finally stained with hematoxylin and eosin.

RESULTS

Gross Observations

The control nerves (Fig. 3) were free of any surgical trauma as expected, and the contours were smooth and symmetric. In contrast, all traumatized nerves presented a range of morphological changes including obvious neuromas (Fig. 3) at the site of injury to no visible changes to the tissue, albeit the latter outcome was uncommon. Neuromas are the result of significant trauma to nerve tissue and are identified by the enlarged bulbous tissue at the site of injury [8,9]. Over 65% of injured nerves showed some evidence of trauma on inspection. Neuromas were seen in all three injury groups, though they were more commonly found in ligated nerves and least common in simple crush injury specimens. It should be noted that 4 of the 12 ligated nerves did not successfully reinnervate the distal segment. Eleven animals also did not survive anesthesia following surgery.

OCT Images

A total of 68 nerves, 34 control and 34 experimental, were imaged using high-resolution OCT at three locations (proximal to injury, injury site, and distal to injury) resulting in a total of 204 (68 nerves × 3 locations) specimens imaged. In each location, multiple OCT sections were obtained to facilitate registration with histologic images. In control specimens, OCT images (Fig. 4) revealed homogenous signal distribution to a relatively uniform depth of roughly 0.25–0.35 mm. This structural pattern was seen in control specimens for all survival times, and the nerve contour appeared smooth. Control nerves did not undergo any injury beyond simple surgical exposure of the intact sciatic.

In contrast, all traumatized nerves (Fig. 5) showed a heterogeneous signal intensity with an increased irregularity at the sites of nerve injury and in distal segments. Similarly, this signal pattern appeared to increase over time. OCT images of the ligated and microsurgically repaired nerves showed the marked signal heterogeneity in the nerve bundle at week 24. For crush injury specimens, the signal heterogeneity was greatest at week 15. Of the three injury models, crush injuries were the least severe, as the endoneurial channels were in theory not severed, and a very modest degree of axonal continuity was maintained. In all three injury groups changes in nerve contour were observed and may reflect the combined effects of inflammation and wound-healing mechanisms.

Histology

Although OCT analysis was comprehensive, histological processing was limited purely for practical reasons. Hence, one nerve was randomly selected from each of the three experimental groups at each specific survival duration (4, 15, and 24 weeks) for a total of nine nerves. Similar to the OCT imaging procedure, each nerve was processed and then transversely sectioned at three locations (proximal to injury, injury site, and distal to injury—three tissue blocks per nerve). In addition to the nine experimental nerves, two control nerves were sectioned ultimately resulting in a total of 33 tissue blocks (11 nerves × 3 locations). For all specimens, a large section of the nerve was harvested in order to insure the histologic sections were in registry with regions imaged using OCT. As such, dozens of individual sections were obtained for each nerve, and surface contour features were used as a guide to maintain registry, in addition to correlation with photographs of the nerve before embedding.

Histological examination of the injured nerves (Fig. 6) showed an increase in connective tissue at the site of injury and distally. The amount of this scar tissue increased with time for all injury

groups. Scar tissue formation may be due to foreign body reactions elicited from the presence of sutures. Such connective tissue was seen in the control group, but unlike the injured groups, the amount observed in the controls was consistent throughout each region (proximal, middle, distal). Histology of the controls showed nerve fibers neatly enclosed in fascicles with minimal surrounding connective tissue. In contrast, the injured/repaired nerves exhibited irregular fascicles, which lack the smooth, circular structure as seen in controls. Furthermore, these fascicles were more densely packed and appeared to progressively decrease in diameter in correlation with increasing time and sectioning distal to injury. Our observations correlated with Ronchi et al [10] who found the regenerated rat median nerve fibers were smaller and more densely packed after crush injury.

Comparison of OCT to Histology

OCT clearly provided information on the structure of a peripheral nerve, though signal intensity diminished with depth. This penetration appeared to be further reduced by the presence of scar tissue. Analysis of histologic sections allowed for identification of structures seen with OCT, and what were initially identified as irregular nerve bundles were in fact regions of *scar* tissue and perineurium. For the injured nerves which developed significant scar tissue during the nerve repair process, it was difficult to obtain images that reflected changes in the underlying nerve bundles. In contrast, in specimens lacking scar tissue, OCT identified microstructural features in the nerves consistent with perineurium, the outer most nerve layer which surrounds and protects nerve fiber bundles (Fig. 7).

DISCUSSION

This study demonstrates the potential for OCT as a high-resolution imaging modality for use in monitoring nerve injury and repair. While current systems are limited in capability, with increased resolution, OCT may supply physicians with real-time images of changes in nerve microstructure that occur following injury, treatment, and repair. This technology may aid physicians in providing quantitative information on nerve growth and repair dynamics.

Although current OCT lacks the resolution to image individual axons, information on nerve contour and appearance of scar tissue may still be of clinical value to help monitor injury and repair in peripheral nerve surgery, even though the imaging depth is limited. As OCT resolution continues to improve, this technology may have the potential to replace nerve biopsies which are occasionally needed to diagnosis peripheral neuropathies. The most common example is sural nerve biopsy which is performed in diabetic patients.

OCT is a valuable imaging tool due to its capability to provide high-resolution cross-sectional images of living tissues. Common imaging modalities including computed tomography (CT), magnetic resonance imaging (MRI), and ultrasound also image subsurface soft tissue structures but lack the resolution necessary to image nerve microstructure [11–14]. Currently, only OCT combines high-resolution and tissue penetration depth required to image nerve microstructures.

Presently, OCT is being utilized in multiple specialties and has had the greatest impact in ophthalmology where it is able to provide cross sections of the optic disc aiding in the diagnosis and monitoring of glaucoma, and in imaging the retina itself [15–17]. Similarly, physicians use OCT to detect abnormal cell development in the human airway, gut, oral cavity, cardiovascular system, and urinary system [18–21].

This study is the first to investigate the peripheral nerve injury and repair process using OCT imaging technology in combination with histological processing. In general, OCT imaging of the injured nerve resulted in heterogeneous signal distribution with an increase signal irregularity at the segments distal to injury site. In contrast, the control nerves presented

homogenous signal distribution to a relatively uniform depth. OCT supplied further information in regard to nerve contour.

Several challenges were encountered while conducting this study. The limited penetration depth prevented imaging beyond the connective tissue surrounding the nerve. Prior to comparison with histology, when only examining OCT images alone, we suspected the irregular signal distribution seen on OCT reflected the irregular nerve bundle geometry resulting from the nerve injury repair process; however, this appears not to be the case. Histological analysis proved this “irregular signal distribution” was actually fibrosis at the injury site. An additional challenge involved the difficultly of obtaining registered histology sections at the precise OCT imaging site. Great care was taken to mark the imaged location; nevertheless, after histological processing and sectioning, determining the exact OCT imaging site was a challenge.

With further advances in OCT imaging technology, specifically improvements in the depth of penetration and resolution, this imaging modality has the potential to be a useful tool providing physicians with a mechanism to visualize structural changes to nerve microstructures.

CONCLUSION

The potential to perform non-invasive, high-resolution in vivo imaging could radically alter nerve injury diagnosis, therapy, and management. We have demonstrated the first OCT images of peripheral nerve in an injury and surgical repair model, and our results suggest that OCT may eventually have some value in diagnosing and monitoring nerve injury, potentially being used as an intraoperative imaging modality. Future studies will focus on OCT devices with improved resolution, higher speed, and greater penetration depth.

Acknowledgments

Contract grant sponsor: U.S. Air Force Office of Scientific Research (Medical Free-Electron Laser Program); Contract grant number: FA9550-04-1-0101; Contract grant sponsor: LAMMP; Contract grant number: RR01192; Contract grant sponsor: National Institute of Health (NIH); Contract grant numbers: EB-00293, CA-91717, RR-001192; Contract grant sponsor: AMA Seed Grant; Contract grant number: AMA-36687; Contract grant sponsor: 2008 ASLMS/U.S. Air Force Travel Grant.

The authors would like to thank Laurie Newman for her help with animal handling and preparation. This work was supported by the U.S. Air Force Office of Scientific Research, Medical Free-Electron Laser Program (FA9550-04-1-0101), LAMMP (RR01192), National Institute of Health (NIH; EB-00293, CA-91717, RR-001192), AMA Seed Grant AMA-36687, and 2008 ASLMS/U.S. Air Force Travel Grant.

References

1. Burnett MG, Zager EL. Pathophysiology of peripheral nerve injury: A brief review. Neurosurg Focus 2004;16(5):1–7. [PubMed: 15254983]
2. Seddon HJ. Three types of nerve injury. Brain 1943;66(4):237–288.
3. Sunderland S. The anatomy and physiology of nerve injury. Muscle Nerve 1990;13(9):771–784. [PubMed: 2233864]
4. Sunderland S, Bradley KC. Denervation atrophy of the distal stump of a severed nerve. J Comp Neurol 1950;93(3):401–409. [PubMed: 14803568]
5. Lundborg G. A 25-year perspective of peripheral nerve surgery: Evolving neuroscientific concepts and clinical significance. J Hand Surg Am 2000;25(3):391–414. [PubMed: 10811744]
6. Huang D, Swanson EA, Lin CP, Schuman JS, Stinson WG, Chang W, Hee MR, Flotte T, Gregory K, Puliafito CA, Fujimoto JG. Optical coherence tomography. Science 1991;254(5035):1178–1181. [PubMed: 1957169]

7. Bourquin S, Aguirre A, Hartl I, Hsiung P, Ko T, Fujimoto J, Birks T, Wadsworth W, Bünting U, Kopf D. Ultrahigh resolution real time OCT imaging using a compact femto-second Nd:Glass laser and nonlinear fiber. Opt Express 2003;11(24):3290–3297. [PubMed: 19471457]
8. Kocsis JD, Preston RJ, Targ EF. Retrograde impulse activity and horseradish peroxidase tracing of nerve fibers entering neuroma studied in vitro. Exp Neurol 1984;B85(2):400–412. [PubMed: 6745381]
9. Kohama I, Ishikawa K, Kocsic JD. Synaptic reorganization in the substantia gelatinosa after peripheral nerve neuroma formation: Aberrant innervation of lamina II neurons by Aβ afferents. J Neurosci 2000;20(4):1538–1549. [PubMed: 10662843]
10. Ronchi G, Nicolino S, Raimondo S, Tos P, Battiston B, Papalia I, Varejão AS, Giacobini-Robecchi MG, Perroteau I, Geuna S. Functional and morphological assessment of a standardized crush injury of the rat median nerve. J Neurosci Methods 2009;179(1):51–57. [PubMed: 19428511]
11. Black PM, Moriarty T, Alexander E 3rd, Stieg P, Woodard EJ, Gleason PL, Martin CH, Kikinis R, Schwartz RB, Jolesz FA. Development and implementation of intraoperative magnetic resonance imaging and its neurosurgical applications. Neurosurgery 1997;41(4):831–845. [PubMed: 9316044]
12. Goldberg BB, Liu JB, Merton DA, Feld RI, Miller LS, Cohn HE, Barbot D, Gillum DR, Vernick JJ, Winkel CA. Sonographically guided laparoscopy and mediastinoscopy using miniature catheter-based transducers. J Ultrasound Med 1993;12(1):49–54. [PubMed: 8455221]
13. Andrew ER. Nuclear magnetic resonance and the brain. Brain Topogr 1992;5(2):129–133. [PubMed: 1489641]
14. Mahmood U, Ridgway J, Jackson R, Guo S, Su J, Armstrong W, Shibuya T, Crumley R, Chen Z, Wong B. In vivo optical coherence tomography of the nasal mucosa. Am J Rhinol 2006;20(2):155–159. [PubMed: 16686378]
15. Sakata LM, Deleon-Ortega J, Sakata V, Girkin CA. Optical coherence tomography of the retina and optic nerve—A review. Clin Exp Ophthalmol 2009;37(1):90–99.
16. Costa RA, Skaf M, Melo LA Jr, Calucci D, Cardillo JA, Castro JC, Huang D, Wojtkowski M. Retinal assessment using optical coherence tomography. Prog Retin Eye Res 2006;25:325–353. [PubMed: 16716639]
17. Mrugacz M, Bakunowicz-Lazarczyk A. Optical coherence tomography measurement of the retinal nerve fiber layer in normal and juvenile glaucomatous eyes. Ophthalmologica 2005;219(2):80–85. [PubMed: 15802931]
18. Gerkens U, Buellesfeld L, McNamara E, Grube E. Optical coherence tomography (OCT). Potential of a new high resolution intracoronary imaging technique. Herz 2003;28:496–500. [PubMed: 14569390]
19. Hanna N, Saltzman D, Mukai D, Chen Z, Sasse S, Milliken J, Guo S, Jung W, Colt H, Brenner M. Two-dimensional and 3-dimensional optical coherence tomographic imaging of the airway, lung, and pleura. J Thorac Cardiovasc Surg 2005;129:615–622. [PubMed: 15746746]
20. Ridgway JM, Ahuja G, Guo S, Su J, Mahmood U, Chen Z, Wong B. Imaging of the pediatric airway using optical coherence tomography. Laryngoscope 2007;117(12):2206–2212. [PubMed: 18322424]
21. Ridgway JM, Armstrong WB, Guo S, Mahmood U, Su J, Jackson RP, Shibuya T, Crumley RL, Gu M, Chen Z, Wong BJ. In vivo optical coherence tomography of the oral cavity and oropharynx. Arch Otolaryngol Head Neck Surg 2006;132(10):1074–1081. [PubMed: 17043254]

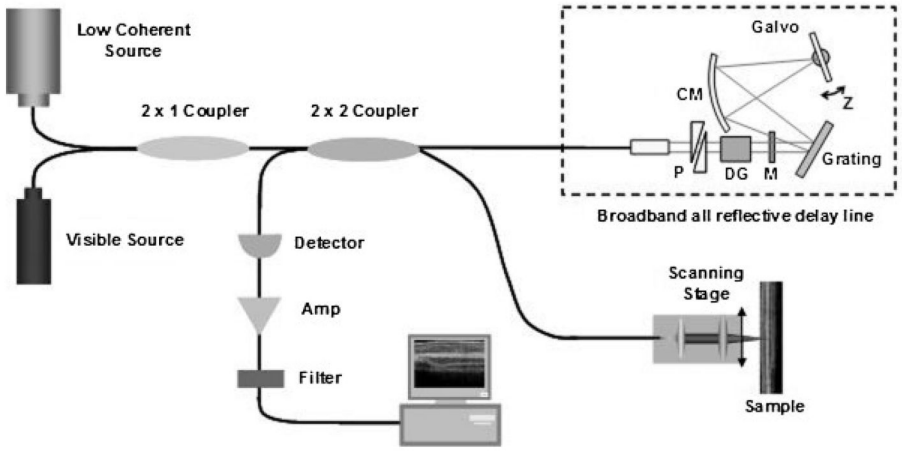

Fig. 1.

Schematic of OCT imaging system. RSOD, rapid-scanning optical delay. Dotted line indicates broadband all reflective delay line. P, prism pair; CM, curved mirror; M, mirror; DG, dispersion compensating glass.

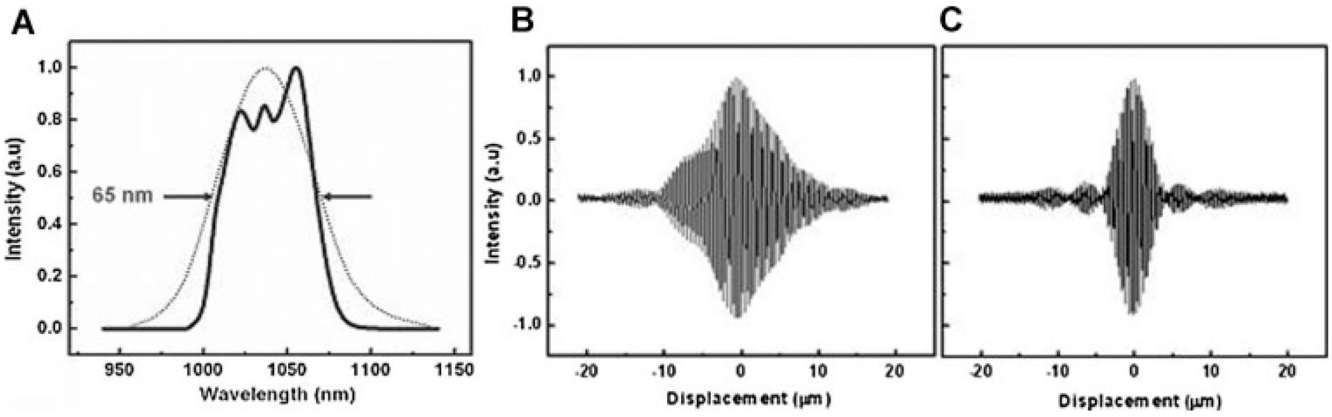

Fig. 2.

A: Spectra of the ASE source. **B**,**C**: Experimental results before and after dispersion compensation. Axial resolution of 7 μm was achieved with precise dispersion matching by means of pair prisms and dispersion compensating.

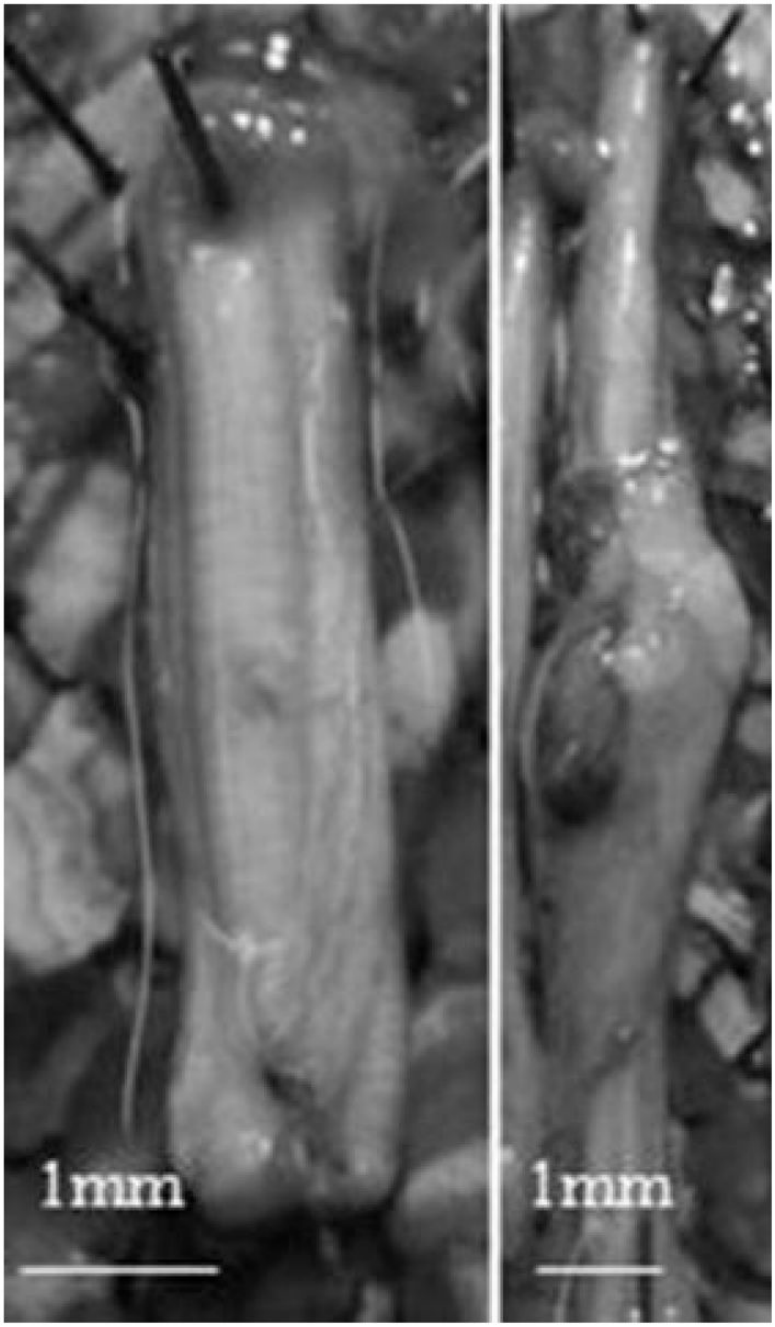

Fig. 3.
Digital images of rat sciatic nerves. Image on the left is of a non-injured control sciatic nerve. On the right, an experimental sciatic nerve developed a neuroma at the injury site.

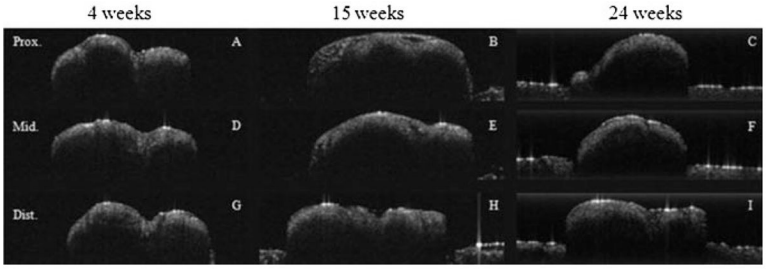

Fig. 4.

OCT images of three separate control (uninjured) sciatic nerves at three time intervals (4, 15, and 25 weeks). All nerves were imaged at three locations: proximal to injury (A–B), injury site/middle (D–F), and distal to injury (G–I). Specimens were scanned 1 mm × 3 mm.

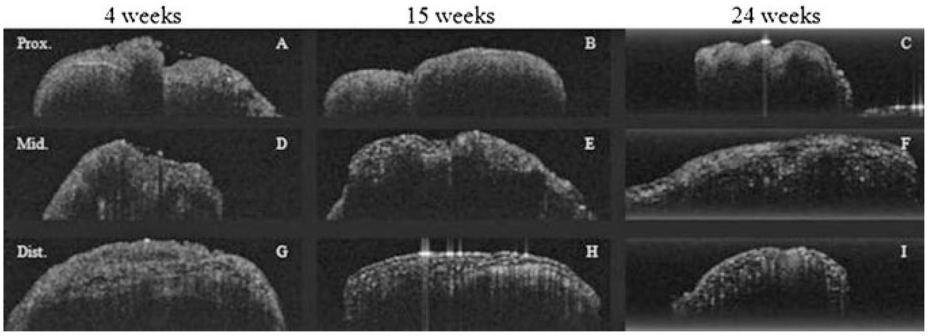

Fig. 5.

OCT images of three separate ligated experimental sciatic nerves at three separate time intervals. All nerves were imaged at three locations: proximal to injury (A–B), injury site/middle (D–F), and distal to injury (G–I). Specimens were scanned 1 mm × 3 mm.

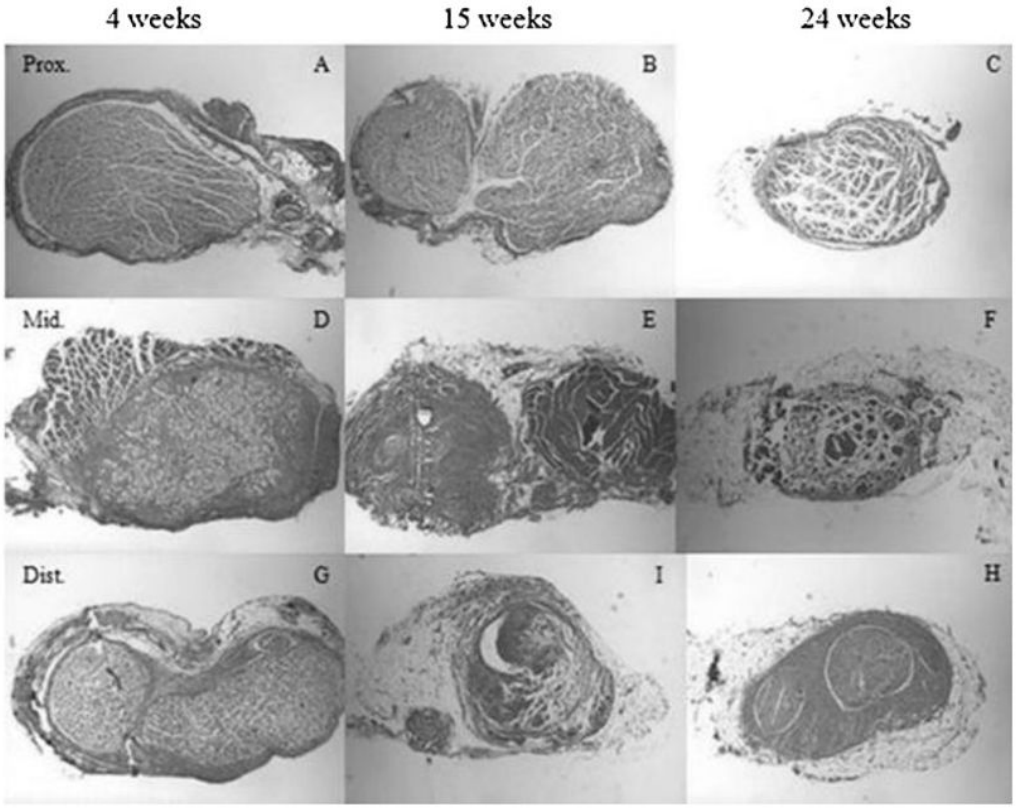

Fig. 6.

Histology of three ligated experimental sciatic nerves at three time intervals. All nerves were sectioned at three locations: proximal to injury (A–B), injury site/middle (D–F), and distal to injury (G–H). The fascicles appeared to progressively decrease in diameter in correlation with increasing time and sectioning distal to injury (original magnification 6.5×).

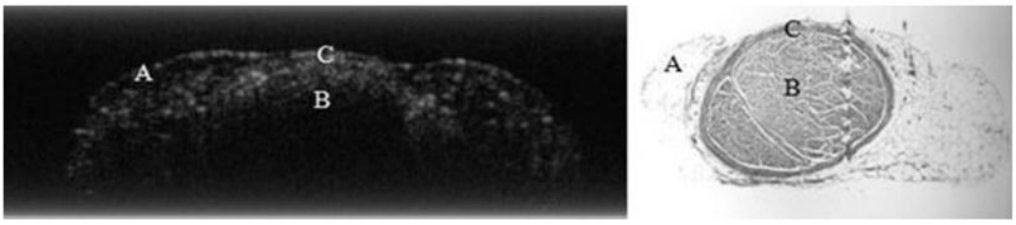

Fig. 7.
The OCT image on the left correlates with the histology section (right) of an injured sciatic nerve. Region “A” highlights connective tissue and “B” signifies nerve fascicle. “C” identifies nerve perineurium (original magnification 6.5×).